String melting of the floating phase in antiferromagnetic clock models

Marcel den Nijs
Department of Physics, University of Washington, Seattle, Washington 98195
(Received 14 June 1984)

In two-dimensional antiferromagnetic q-state clock models with odd values of $q=5,7,9,\ldots$ on a square lattice, the low-temperature phase is a floating solid, with impurities and logarithmically bound vortices. Both are composite objects. Inside their cores they contain vertices of vorticity 0 and $\pm q$ bound together by linear interactions induced by strings. The meander entropy of these strings competes with the positional entropy of the composite vortices. Kosterlitz-Thouless melting is preempted by a string-melting transition, where the cores of the vortices and impurities diverge.

I. INTRODUCTION

In a conventional two-dimensional (2D) floating solid phase, vortex excitations have a small core and are bound in pairs logarithmically. Dislocation melting is driven by their positional entropy: the Kosterlitz-Thouless (KT) transition.[1-3] As shown in this paper, the low-temperature phase of two-dimensional antiferromagnetic (AF) q-state clock models, with odd values of q, is a floating solid which melts via a divergency of the core size of vortices and annealed impurities.

At the smallest length scale the configurations are described by strings and by vertices with vorticity 0 and $\pm q$. The vertices, to be distinguished from vortices, have a fixed core size equal to the lattice constant. A string tension $f_S(i)$ can be associated to each type of string. They define a set of characteristic length scales $l_S(i)\sim f_S(i)^{-1}$. Let $l_S(i)>l_S(i+1)$.

At length scales $l\gg l_S(1)$, the low-temperature phase is a floating solid with annealed impurities, and with logarithmically bound vortices. At length scales $l<l_S(1)$ these vortices and impurities display an internal structure. They are composite objects built from vertices with flux 0 and $\pm q$, glued together linearly by several types of strings. The vortices have total Burgers vector $\pm nq$. n takes a specific value in each corner of the phase diagram. Impurities in the context of this paper are bound groups of vertices with total Burgers vector zero. The string lengths $l_S(i)$ determine the internal structure. If $l_S(2)\gg l_S(i)$ for all $i>2$, the vertices are clustered internally in mq vortices (in general $m<n$).

Two types of entropy compete to melt this type of floating phase. (i) The positional entropy S_P of the composite vortices can lead to KT melting into a fluid with free composite vortices. At the KT transition temperature T_{KT} the positional entropy exceeds the logarithmic interaction energy between the composite vortices. (ii) The meander entropy S_M of the strings inside the vortex and impurity cores can lead to string melting. For each type of string there is a characteristic temperature $T_S(i)$ at which its string tension $f_S(i)$ vanishes. At $T_S(i)$ the meander entropy exceeds the energy of the string (measured with respect to the free energy of the surrounding floating phase). At $T_S(1)$ the cores of the composite impurities and nq vortices diverge. They fall apart in smaller composite impurities and mq vortices, depending on the actual structure inside the core, and the relative values of the remaining string tensions.

Several melting sequences are possible, as outlined below.

(a) Kosterlitz-Thouless melting into an nq fluid. The positional entropy S_P exceeds the logarithmic interaction between the composite vortices, before their cores diverge.

(b) String melting into an mq fluid. The divergence of the cores of the impurities and vortices preempts KT melting. At $T_S(1)$ only the string tension of the least expensive strings vanish. The impurities and nq vortices fall apart in smaller impurities and mq vortices. At length scales $l_S(2)<l<l_S(1)$, the system is in a fluid or a floating solid phase. $T_S(1)$ is the melting temperature if the positional entropy of the mq vortices already exceeds the value where logarithmically bound mq vortex pairs would unbind.

(c) Crossover to a floating phase with logarithmically bound mq vortices. Also in this case $f_S(1)$ vanishes before the positional entropy of the nq vortices becomes large enough to establish a KT transition. But the positional entropy S_P at the next length scale $l_S(2)$ is still smaller than the value where logarithmically bound mq-vortex pairs unbind. $T_S(1)$ is not the melting temperature. The floating phase does not melt. It changes its character. The effective Gaussian coupling constant K, which characterizes S_P, is singular at T_S. Melting, type (a) or (b), takes place at higher temperatures, by excitations at length scale $l_S(2)$, or can be further delayed via another type-(c) crossover inside the floating phase.

(d) Disorder lines. In the fluid phase after the type-(a) or -(b) melting transition, the vortices are free, but like the impurities they are still composite objects. The temperatures $T_S(i)$, where the remaining string tensions vanish, represent disorder lines, where the free vortices and impurities decay further, until the q gas is reached with free (pointlike) q vertices. At a disorder line the fluid changes its character. The correlation length does not diverge. No thermodynamic singularities are expected; at most, a broad maximum in the specific heat may occur if the entropy increases rapidly at the partial breakup of the impurities and vortices. However, one can imagine that in

some cases disorder lines develop into genuine fluid-fluid phase transitions.

The purpose of this paper is to show that in two-dimensional AF q-state clock models with odd values of q, the low-temperature phase is a floating phase as described above, with strings and composite impurities and vortices, and that string melting sequence (b) is realized. It turns out that the description by means of strings, impurities, and vortices explains and/or predicts most properties of the model with a minimum of additional exact, numerical, and analytical information.

Consider the q-state clock model with odd values of q on a square lattice with only nearest-neighbor interactions,

$$H=\sum_{\langle r',r\rangle}\sum_{n=0}^{q-1}J(n)\cos\{n[\theta(r')-\theta(r)]\}\ , \tag{1}$$

where $\theta(r)=2\pi m/q$, $m=0,\ldots,q-1$, and $J(m)=J(q-m)$. The phase diagram will be discussed in the vertex representation. The angle variables $\theta(r)$ are replaced by bond variables

$$d_h(r',r)=-d_h(r,r')=[\theta(r')-\theta(r)]/(2\pi/q)$$

located at the bonds of the dual lattice. Represent $d_h=0$ by the absence of an arrow at the bond (place a zero), $d_h=\pm1$ by single arrows, $d_h=\pm2$ by double arrows, etc. Choose the arrow direction such that while looking along the arrow $\theta(r')-\theta(r)$ rotates clockwise. At each vertex R (site of the dual lattice) the next flux of arrows must be equal to $0 \bmod q$ because

$$\sum_{\mathfrak{P}}[\theta(r)-\theta(r')]=0 \bmod 2\pi\ .$$

The arrows contribute factors $x(d_h)$ to the Boltzmann weight,

$$x(n)=\exp\left[\sum_{m=0}^{q-1}J(m)\cos(2\pi mn/q)\right]\ . \tag{2}$$

In the absence of the vertex states with flux $\pm q$ the model would reduce to a so-called solid-on-solid (SOS) model. The $d_h=0,\pm1,\pm2,\ldots,\pm(q-1)/2$ arrow states would describe steps in a 2D interface. The vertex states with flux $\pm q$ represent screw dislocations in the interface.[4]

In specific corners of the phase diagram a specific subset of steps is most favorable, leading to a specific low-temperature ordered or floating solid phase. Distinguish between favorable steps, unfavorable steps, and vertex states with flux $\pm q$. As described in the next sections, the unfavorable steps represent string excitations within the ordered or floating solid phase, i.e., within the background "sea" of favorable arrow states.

A string tension can be associated to each type of unfavorable step. In ordered phases the correlation length is inversely proportional to the string tension of the cheapest strings. In floating solid phases the correlation length is already infinite.

The lowest excitations are impurities, vortices, and closed loops of strings. The vertex states with flux $\pm q$ combine into impurities and nq vortices, glued together by the strings. In each corner of the phase diagram n has a specific value, and the inside of the cores a specific structure.

It is well known that order-disorder transitions can be presented as a deconfinement of linearly bound dislocations. In the scaling limit at the ordered side, dislocations interact linearly at large distances, $r>\xi$ and logarithmically at short distances $r<\xi$. In the floating phase described here, at temperatures large enough such that all the strings are large with respect to the lattice constant, a sequence of length scales exists. At each, the vertices combine into more complex vortices and neutral impurities. The impurities are always free. Up to the length scale l_M, corresponding to the melting temperature, the vortices are free (the fluid phases; asymptotical freedom). The composite vortices at larger lengths scales $l\gg l_M$ interact logarithmically. The crossover at l_M is described by the KT transition or the string melting transition.

For increasing q the structure inside the vortices and impurities becomes more complex. There are $(q-1)/2$ different types of strings. Along specific paths through the phase diagram, elaborate sequences of disorder lines [sequence (d)] and of boundaries within the floating phase with singularities in the effective Gaussian coupling constant [sequence (c)] might be realized, at the high- and low-temperature side of the string melting [sequence (b)] or KT melting line [sequence (a)], respectively.

In Sec. II the phase diagram of the 5-state clock model is discussed. In Sec. III the results are generalized to odd values of $q>5$. The antiferromagnetic side of the phase diagrams is new. KT melting sequence (a) cannot be ruled out, but string melting sequence (b) is more likely for most paths through the phase diagram. In particular it is shown that string melting sequence (b) is certainly realized at $q=5$ in the SOS model limit. In the same limit for $q>5$ the ferromagnetic (F) and antiferromagnetic (AF) floating phases become directly connected, and sequence (c) is realized.

Also at the ferromagnetic side of the phase diagrams the string language is useful. It predicts the presence of disorder lines, and explains the crossover from the intermediate floating phase (in the SOS model region) to the first-order transition (around the Potts model).

II. 5-STATE CLOCK MODEL

Figure 1 shows the phase diagram for $q=5$ as function of

$$A=x(0)/[x(1)+x(2)]$$

and

$$B=[x(1)-x(2)]/[x(1)+x(2)]\ .$$

$(A,B)=(\frac{1}{2},0)$ represents infinite temperature. The line $B=0$ corresponds to the 5-state Potts model. Along the dashed lines in Fig. 1 the ratio $J(1)/J(2)$ is fixed. The phase diagram has mirror symmetry with respect to the $B=0$ axis; the transformation $\theta\rightarrow-2\theta$ [see Eq. (1)] exchanges $x(2)$ with $x(1)$.

At $B=-1$ the double arrows are frozen out, at $B=1$ the single arrows, and at $A=0$ the zeros. For $A\gg1$ the model is in the ferromagnetic ground state, with only

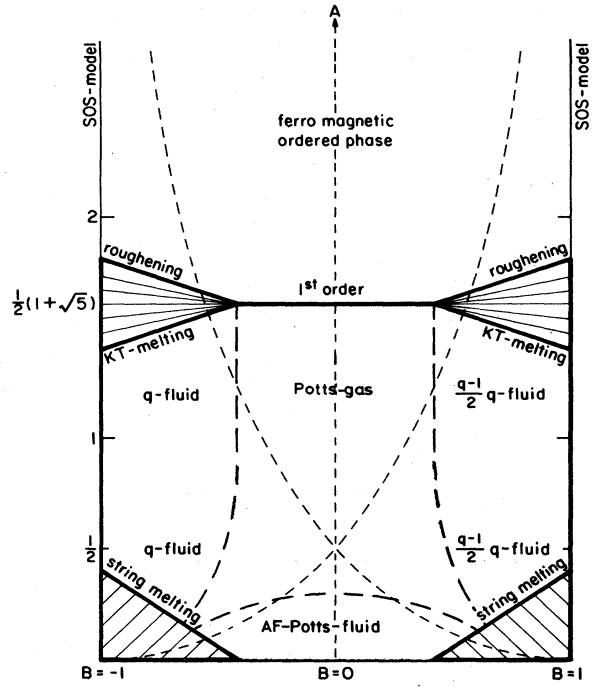

FIG. 1. Schematic phase diagram of the 5-state clock model. The heavy drawn lines represent phase transitions. The heavy dashed lines are disorder lines. The shaded areas are floating phases. The shading follows lines of constant effective Gaussian coupling constants. The light dashed lines represent paths through the phase diagram where the ratios between the coupling constants are fixed.

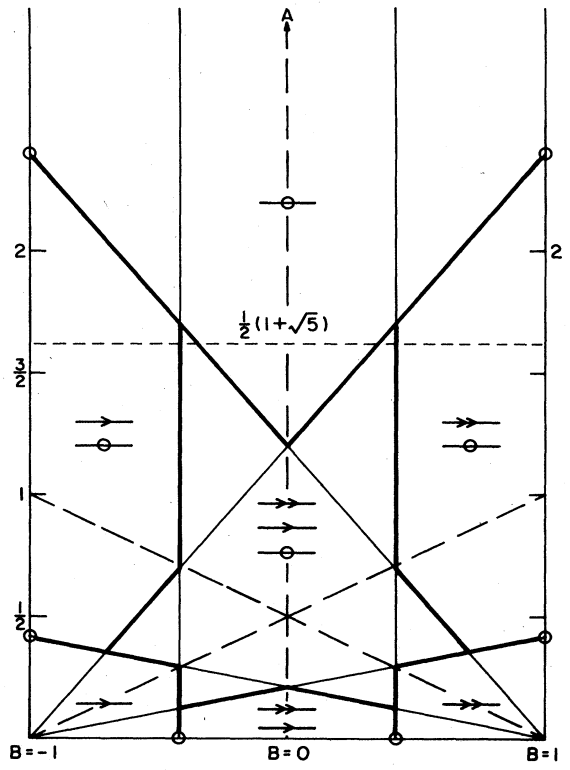

FIG. 2. The seven domains in the 5-state clock model phase diagram. Along the heavy dashed lines two of the three Boltzmann weights are equal, $x(i)=x(j)$. Along the drawn lines $x(i)/x(j)=\sqrt{2}-1$ a single string of type i melts in a sea of strings of type j (see Appendix). The heavy drawn parts approximate the boundaries between the seven domains. Their continuation of the three low-temperature phases indicate a change in the lowest excitations.

zeros. In the AF ground states at $(A,B)=(0,-1)$ and $(A,B)=(0,1)$, only the single arrows or double arrows are allowed. In both cases the model reduces to the 6-vertex model at the so-called ice point where all allowed arrow configurations (those with zero flux at every vertex) have equal Boltzmann weight. At the ice point the 6-vertex model, and therefore also the AF clock model at zero temperature is in its floating solid phase.

The basic idea is to describe the melting of these three low-temperature phases from the point of view of strings and vortices, using exact and numerical information for the positional entropy S_P, and a single-string approximation (see Appendix) for the meander entropy S_M.

From the point of view of the strings the phase diagram contains seven different domains. In each the set of favorable and unfavorable steps is different. Figure 2 illustrates this. Along the dashed lines two of the Boltzmann weights are equal, $x(i)/x(j)=1$. At the drawn lines $x(i)/x(j)=\sqrt{2}-1$ a single string of type i would melt (because of its meander entropy) in a background sea with only steps of type j (see Appendix). These lines give only crude estimates of the boundaries (the fat drawn segments) between the seven domains. Around the encircled points the approximation must be reasonable. The continuation of the drawn lines inside the three low-temperature phases separate regions where the nature of their lowest excitations changes.

A. Ferromagnetic side of the phase diagram

As is well known the ferromagnetic order-disorder transition in the $q>4$ state Potts model is first order,[5] and remains first order also in the direct vicinity of $B=0$. The transition takes place at the self dual line $A^*=(1+\sqrt{q})2/(q-1)$. For general q the duality equations are[3,6]

$$x(n)'=q^{-1/2}\sum_{m=0}^{q-1}x(m)\exp(inm2\pi/q)\,, \tag{3}$$

for $q=5$; in the (A,B) parametrization, they read

$$A'=(A+2)/(2A-1)\,,$$
$$B'=\sqrt{5}B/(2A-1)\,. \tag{4}$$

At the first-order line the ordered phase melts directly into a Potts gas with free q vertices (see also below). First we will discuss the phase diagram around $B=-1$ then around $B=1$ and finally will return to $B=0$ (compare with Fig. 2).

In the $B=-1$ region the ferromagnetic ordered phase

melts via an intermediate floating phase by two KT transitions.[3,7]

Along the line $B=-1$ (where double-arrow states are frozen out), the model reduces to the so-called restricted SOS model, which describes a 2D interface. $h(r)=\theta(r)/(2\pi/q)$ represents the height of a column of atoms. Vertex states with flux $\pm q$ [Fig. 3(a)] are frozen out. The mod2π character of the angle variables $\theta(r)$ can be ignored, because the Burgers vector $\sum_{\rho} d_h$ is equal to zero along every contour. Since nearest-neighbor columns can only differ by $d_h(r',r)=0,\pm 1$, this is known as the restricted SOS model. Each $d_h=0$ contributes a factor $A=x(0)/x(1)$ to the Boltzmann weight and each step $d_h=\pm 1$ a factor 1. Finite-size-scaling calculations locate the roughening transition at $A_R=1.8$.[8] Above the roughening temperature $A<A_R$, the rough interface can be characterized by its effective Gaussian coupling constant K,

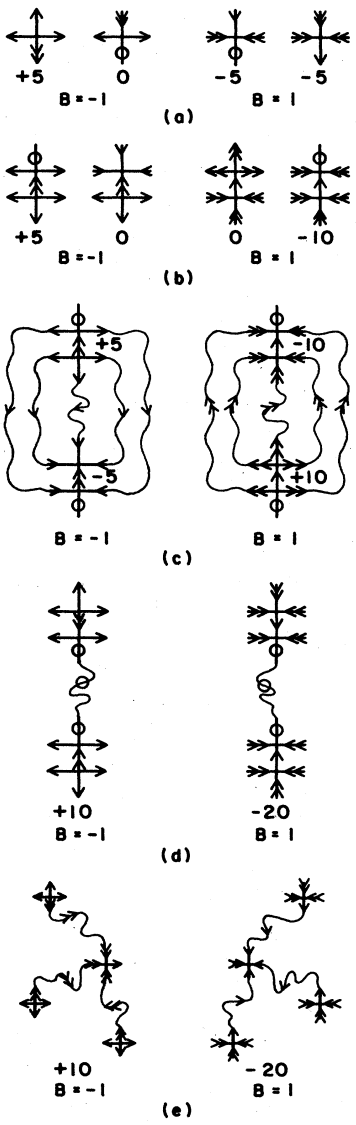

FIG. 3. Composite vortices in the 5-state clock model.

$$\langle [h(r+r_0)-h(r_0)]^2\rangle \simeq (\pi K)^{-1}\ln(r), \quad \text{for } r \gg l_S(1) . \tag{5}$$

K decreases monotonically with temperature. Since the roughening transition is driven by the spin-wave operator $\cos(2\pi h)$, K has the universal value $K_R=\pi/2$ (Refs. 2 and 9) at the roughening temperature. At the self-dual line K has the universal value $K^*=2\pi/q$.[3] From the point of view of the SOS model, vertex states with flux $\pm q$ introduce screw dislocations.[4] These vortices do not appear as free vertex states of flux $\pm q$. Each q vortex and each impurity is a bound pair of vertex states with flux $\pm q$ or flux 0 [Fig. 3(b)], which have in common that they are sinks for double arrows [Fig. 3(a)]. Each pair is bound linearly by a short string of double arrows. The core size is inversely proportional to the string tension of the double arrows.

Below the roughening transition also the single-arrow strings have a finite string tension. In the ordered phase the typical configuration is a sea of zeros, with as lowest excitations: small closed loops of single arrows $d_h=\pm 1$, free impurities, and 5-vortices [Fig. 3(b)]. The 5-vortices are bound together linearly in neutral $(+5)$—(-5) pairs by strings of single arrows [Fig. 3(c)]. The correlation length is inversely proportional to the string tension of the single arrows. The double-arrow strings have a much larger string tension and only appear inside the core of the vortices.

At the roughening transition into the intermediate floating phase (Fig. 1), the correlation length diverges exponentially.[2] The string tension of the single arrows vanishes but the string tension of the double arrows remains. The single-string approximation discussed in the Appendix predicts that the single arrows melt at $A_S\simeq 1+\sqrt{2}$. The approximation overestimates the string entropy. Actually this value of A is close to the location of the broad maximum in the specific heat just below the roughening transition predicted by renormalization transformations.[2] From the point of view of the strings, the maximum is due to a rapid increase of the string length. The single-string approximation predicts that the length of the single-arrow strings only increases rapidly very close to A_S (see Appendix). This increase slows down just before the string tension vanishes because of mutual screening.

In the intermediate floating phase, $A_{\rm KT}<A<A_R$, the typical configuration is a sea of zeros and single arrows, with free impurities, and with 5-vortices. The massless spin-wave excitations, i.e., the fractal structure of the single-arrow strings, keep the $(+5)$—(-5) vortex pairs bound logarithmically. (The distribution of the string, the probability that the string extends in space over a distance r from the vortex pair, decays as a power law. Pulling at the two ends of the string gives a logarithmic response.) Still the double arrows only appear inside the vortex cores.

The effective Gaussian coupling constant is a measure for the positional entropy S_P. At $K=K_{\rm KT}=8\pi/q^2=8\pi/25$,[1,3] the $(+5)$—(-5) vortex pairs unbind. Their positional entropy exceeds the logarithmic string energy. The finite-size scaling calculation for the restricted SOS model by Luck[10] implies that $K(1,-1)=0.86$ [the point $(A,B)=(1,-1)$ represents infinite temperature

in the restricted SOS model]. Because this value is smaller than K_{KT}, the KT melting line ends at $A_{KT}>1$. Notice that the line $A=(\sqrt{5}B+1)/2$ is dual to the line $B=-1$ [Eq. (4)]. Therefore Luck's[8] result for the roughening temperature A_R in the restricted SOS model also gives a point on the KT melting line, $(A,B)=(1.46,-0.86)$.

In the q fluid at $A<A_{KT}$ the typical configuration is a sea of zeros, single arrows, free impurities, and free 5-vortices [Fig. 3(b)]. (The strings of single arrows between each vortex pair are evenly distributed over space. It does not use any free energy to pull their ends further apart.) The string tension of the double arrows remains nonzero.

The description of the $B>0$ region is more complicated but consistent with $B<0$, as required by the $\theta\rightarrow-2\theta$ symmetry. At $B=1$ the model reduces again to the restricted SOS model. The vertex states with flux $\pm q$ are again frozen out. This time, because step sizes $d_h=0, \pm(q-1)/2$ cannot give rise to odd Burgers vectors. According to Eq. (5), the Gaussian coupling constant is four times smaller because the step size $(q-1)/2$ is 2 times larger:

$$K(A,B)=[2/(q-1)]^2K(A,-B) \text{ for } B>0 .$$

From this point of view the roughening transition at $A_R=1.8$ is driven by the spin-wave operator $\cos\{[2/(q-1)]2\pi h\}$, which indeed predicts a universal value

$$K_R=[2/(q-1)]^2\pi/2=\pi/8 ,$$

four times smaller than at $B=-1$. At the self-dual line, K has the universal value

$$K^*=[2/(q-1)]^2 2\pi/q=\pi/10 .$$

Around $B<1$ the q vertices again only appear in groups, but now with a net vorticity 0 or $\pm q(q-1)/2$ [Fig. 3(b)]. Each impurity and 10-vortex is a bound pair of two vertex states with flux ± 5. Each is a sink for single arrows [Fig. 3(a)]. The pair is bound linearly by a short string of single arrows. The core size is inversely proportional to the string tension of the single arrows. The transformation $\theta\rightarrow-2\theta$ maps a 5-vortex at $B=-1$ into a 10-vortex at $B=1$ [Fig. 3(b)]. The single-arrow string must be present, because if the total vorticity encircled by a contour is odd, then at least one single-arrow state must pierce through it (for general q at least one odd step). In this part of the phase diagram, single arrows have the largest string tension and only appear inside the core of the impurities and 10-vortices.

Below the roughening temperature the double-arrow strings have a finite string tension too. For $B>0$, the typical low-temperature configuration is again a sea of zeros, but with different low-lying excitations. It contains small loops of double arrows, free impurities, and 10-vortices. The 10-vortices are bound linearly in neutral $(+10)$—(-10) pairs by strings of double arrows [Fig. 3(c)]. At A_R, the string tension of the double arrows vanishes, while the string tension of the single arrows remains. In the floating phase the typical configuration is a sea of zeros and double arrows, with free impurities and with 10-vortices. The massless spin-wave excitations, i.e., the fractal structure of the double-arrow strings keeps the 10-vortices bound together logarithmically.

At

$$K_{KT}=8\pi/[q(q-1)/2]^2=8\pi/100 ,$$

the positional entropy unbinds the $(+10)$—(-10) pairs [Fig. 3(c)]. At this KT transition K is indeed four times smaller than at $B<0$. In the $q(q-1)/2$ fluid the typical configuration is a sea of zeros and double arrows, with free impurities and free 10-vortices [Fig. 3(b)]. The double-arrow strings are evenly distributed over space. The string tension of the single arrows remains nonzero.

The fluid phases change into a Potts gas with free q-vertices [Fig. 3(a)] in the $B=0$ region. In the $q(q-1)/2$ fluid, the string tension of the single arrows has not vanished yet. It binds q-vertices together in free impurities and free 10-vortices [Fig. 3(b)]. The core size is inversely proportional to the string tension of the single arrows. The $q(q-1)/2$ fluid transforms into a Potts gas at the disorder line where the string tension of the single arrows vanishes.

On the other hand, in the q fluid, the string tension of the double arrows has not vanished yet. The q fluid with free impurities and free 5-vortices [Fig. 3(b)] transforms into the Potts gas at the disorder line where the string tension of the double-arrow strings vanish. In the Potts gas the typical configuration is a sea of zeros, single and double arrows, and free q-vertices [Fig. 3(a)].

At the disorder lines the correlation length does not diverge. Only a broad maximum in the specific heat can be expected, due to a rapid increase in entropy from the unbinding of the impurities and vortices [Fig. 3(b)] into free q-vertices [Fig. 3(a)]. Also, the renormalization transformation for the planar model[2] predicts a maximum in the specific heat at the fluid side just after the KT transition. In the planar model the vortices have fixed-core sizes. The maximum is associated to a rapid increase of entropy due to the unbinding of the logarithmically bound vortex pairs [the dual effect of the rapid increase of the string length just below the roughening transition; see Eq. (3)]. The two effects give rise to two distinguishable maxima or smear out into one broad maximum.

In the $B=0$ region the floating phases do not appear. The ferromagnetic solid phase melts directly into the Potts gas via a first-order transition. Notice that around $B=0$ the (now very crude) single-string approximation predicts string melting beyond the self-dual line (Fig. 2). The point where the $x(1)/x(0)=\sqrt{2}-1$ line and the $x(2)/x(1)=\sqrt{2}-1$ line cross gives a zeroth-order estimate of the value of B at the self-dual line where the critical fan closes, i.e., where the floating phase is replaced by the first-order line, $|B|\simeq\sqrt{2}-1$.

B. Antiferromagnetic side of the phase diagram

At the antiferromagnetic side the vortices and impurities become more complex. Moreover, the restricted SOS models at $B=\pm1$ become "antiferromagnetic." Again the $B=-1$ region is discussed first, followed by the $B=1$ re-

gion and finally the $A=0$ region.

For $A<1$ the $B=-1$ region describes an antiferromagnetic (AF) restricted SOS model with screw dislocations. Steps $d_h=\pm 1$ are more favorable than zeros $d_h=0$. At zero temperature $(A,B)=(0,-1)$ both the double arrows and the zeros are frozen out. The model reduces to the 6-vertex model [also known as the BC-SOS (body-centered—solid-on-solid) model] at the so-called ice point where all Boltzmann weights are equal. The interface is still rough, since $K(0,-1)=\pi/6$.[11] The AF-restricted SOS model remains in the floating phase at all temperatures, and K increases monotonically with temperature, $\pi/6<K<0.86$. The roughness of the interface increases at lower temperatures. At first this sounds counter intuitive, but is obvious from the fact that at lower temperatures the zeros, which make the interface more rigid, become less likely.

Steps of height $d_h=\pm 2$ on the other hand soften the elastic constant of the interface. Therefore K decreases with B. The shading inside the floating phases in Fig. 1 indicates lines of constant K. Along a path where the ratios between the coupling constants $J(n)$ are fixed the interface roughness is likely to increase with temperature.

The q-vortices [Fig. 3(b)] are bound in pairs by strings of zeros [Fig. 3(d)]. The background sea now consists of single-arrow strings. The strings of zeros are present because the vorticity is odd, while every contour on the (square) lattice intersects an even number of bonds. If the total enclosed Burgers vector is odd, at least one zero or double arrow must pierce through the contour (for general q at least one even step).

At first the strings look like a peculiarity of the square lattice. For example, it seems as if the strings are absent in a clock model at a triangular lattice. There the arrows are located at a honeycomb lattice (the dual lattice), and the contours can intersect an odd number of bonds. The situation is more complex however, because it is impossible to draw a configuration with only single arrows (the number of bonds at each vertex is odd). In this paper the discussion is restricted to the square lattice.

The low-temperature floating phase has the properties discussed in the Introduction: The typical configuration is a sea of single arrows, with massless spin-wave excitations (fractal meanders of single-arrow steps), small closed loops of zeros, free impurities, and logarithmically bound $(+10)$—(-10) vortex pairs. The core of the impurities and 10-vortices consist of two 5-vortices [Fig. 3(b)] bound linearly by a string of zeros [Fig. 3(d)]. The 10-vortices are bound in neutral pairs logarithmically by fractal strings of single arrows. Close to $B=-1$ the presence of the double arrows remains restricted to the core of the 5-vortices.

Along a path with fixed B and increasing A the positional entropy S_P and meander entropy S_M do not compete; the string tension of the zeros becomes smaller but K increases with temperature. The single-string approximation discussed in the Appendix predicts that the string tension of the zeros vanishes at $A_S=\sqrt{2}-1=0.414$. At A_S the floating solid melts into a q fluid, by string melting sequence (b).

On the one hand Luck's numerical result $K(1,-1)=0.86$ excludes the possibility of sequence (c), because this value of K at $(A,B)=(1,-1)$ is the upper bound for all $A<1$. At A_S, and everywhere else for $A<1$, K is smaller than the value $K_{\mathrm{KT}}=8\pi/25$, where logarithmically bound $(+5)$—(-5) vortex pairs would unbind. Therefore the 5-vortices are free inside the 10-vortex and impurity cores.

On the other hand, the exact result $K(0-,1)=\pi/6$ excludes KT melting sequence (a), because the value of K at $(A,B)=(0,-1)$ is a lower bound for all A close to $B=-1$. At A_S, and everywhere else around $B=-1$, K is larger than $K_{\mathrm{KT}}=8\pi/100$ where the logarithmically bound $(+10)$—(-10) vortex pairs unbind.

Therefore string melting sequence (b) from the floating solid into the q fluid must be realized in the SOS model limit, close to $B=-1$. Notice that the F and AF floating phases are disconnected (Fig. 1).

Again the description in the $B=1$ region, although more complicated, is consistent with $B<0$. Also the restricted SOS model at $B=1$ becomes antiferromagnetic. According to (5) $K(0,1)=[2/(q-1)]^2\pi/6$ is four times smaller than at $(A,B)=(0,-1)$. Again K increases monotonically with temperature, since zeros decrease the height fluctuations.

As in the ferromagnetic domain, the q-vertices are strongly bound in impurities and in vortices with flux $\pm q(q-1)/2$ by a short string of single arrows [Fig. 3(b)]. At larger length scales these $q(q-1)/2$-vortices are bound together in neutral impurities or vortices with flux $\pm 2q(q-1)/2$, by longer (weaker) strings of zeros [Fig. 3(d)]. The transformation $\theta\rightarrow -2\theta$ maps a $(+5)$—$(+5)$ vortex pair at $B=-1$ into a (-10)—(-10) vortex pair at $B=1$ [Fig. 3(d)]. The strings are present, because the vorticity $q(q-1)/2$ is not an even multiple of the step size $(q-1)/2$, while each contour on the (square) lattice intersects an even number of bonds. If the total enclosed Burgers vector is not an even multiple of $(q-1)/2$, then at least one step different from $\pm(q-1)/2$ must pierce through the contour.

Again the low-temperature floating phase has the properties described in the Introduction: The typical configuration is a sea of double arrows, with massless spin-wave excitation (fractal meanders of double-arrow steps), small closed loops of zeros, free impurities, and logarithmically bound $(+20)$—(-20) vortex pairs. The cores of the impurities and 20-vortices [Fig. 3(d)] consist of two 10-vortices [Fig. 3(b)] bound linearly by a string of zeros. Moreover these 20-vortices are bound in neutral pairs logarithmically by fractal structured double-arrow strings. Close to $B=1$ the presence of the single arrows remains restricted to the core of the 10-vortices.

At the string-melting line the floating phase melts into a $q(q-1)/2$ fluid. Again the possibility of sequence (c) is excluded because the value $K(1,1)=0.22$ at $(A,B)=(1,1)$ is the upper bound for all $A<1$, $B>0$, and smaller than $K_{\mathrm{KT}}=8\pi/100$ where logarithmically bound (10)—(-10) vortices unbind. After the string tension vanishes, the 10-vortices are free. Again KT melting, sequence (a) is excluded because $K(0,1)=\pi/24$ is the lower limit of K around $B=1$, and is larger than $K_{\mathrm{KT}}=8\pi/400$, where the logarithmically bound (20)—(-20)

vortex pairs would unbind.

Hence, string melting sequence (b) into the $q(q-1)/2$ fluid must be realized close to $B=1$. Indeed the results are completely symmetric with respect to the $B=-1$ region.

In the $A=0$ region the zeros are the most favorable states. The AF five-state Potts model at $B=0$ is believed to remain disordered at all temperatures. The floating phases at $A=0$ melt before (or at) $B=0$. The behavior along $A=0$ is more characteristic for paths with fixed $J(2)/J(1)$ ratios than the behavior along $B=\pm 1$ (Fig. 1).

If vortices could be ignored, the model would transform continuously from a BC-SOS model with only $d_h=\pm 1$ steps, into a BC-SOS model with only $d_h=\pm(q-1)/2$ steps. This suggests that K decreases monotonically from $K(0,-1)=\pi/6$ to $K(0,1)=[2/(q-1)]^2\pi/6$. However, the $\theta\rightarrow -2\theta$ symmetry implies that $K(A,-B)=4K(A,B)$ (for $B>0$). K is not a monotonic function of B, but decreases with B for $B<0$, and increases with B for $B>0$. Vortices [Fig. 3(e)] renormalize K to a smaller value by an amount proportional to their fugacity $1\pm B$.[2] This renormalization is considerable because it must overtake the monotonic behavior. Around $B=0$ the effective Gaussian coupling constant might become very small.

The rate by which $K(0,B)$ decreases is crucial. In contrast to the $B=\pm 1$ region, KT melting sequence (a) and string melting sequence (b) compete.

In the floating phase around $B=-1$ the typical configuration is a sea of single arrows with massless spin-wave fluctuations. It contains small closed loops of double arrows, free impurities, and logarithmically bound 10-vortices. The cores of the 10-vortices and impurities are more complicated now, because they consist of q-vertices glued together by double arrows only [Fig. 3(e)]. KT melting sequence (a) preempts string melting sequence (b) if K becomes smaller than $K_{\mathrm{KT}}=8\pi/100$ before the string tension of the double arrows vanishes. String melting leads directly to the AF Potts fluid with free q-vertices but no zeros. KT melting sequence (a) into a $2q$ fluid with free 10-vortices [Fig. 3(e)] would be followed by a disorder line into the AF Potts fluid.

In the floating phase around $B=1$ the typical configuration is a sea of double arrows with massless spin-wave fluctuations. It contains small closed loops of single arrows, free impurities, and logarithmically bound $(+20)$—(-20) vortices. The cores of the impurities and 20-vortices consist of q-vertices glued together by single-arrow strings [Fig. 3(e)]. KT melting sequence (a) preempts string melting sequence (b) if K becomes smaller than $K_{\mathrm{KT}}=8\pi/400$ before the string tension of the single arrows vanishes. String melting sequence (b) would lead directly to the AF Potts fluid with free vertex states with flux $\pm q$ but no zeros. KT melting sequence (a) into the $2q(q-1)/2$ fluid [Fig. 3(e)] would be followed by a disorder line into the AF Potts fluid.

No additional information about the variation of K along the $A=0$ is available. The single-string approximation predicts that the string tension vanishes at $|B_S|=1-\sqrt{2}$. K must decrease by more than a factor of 2 between $B=-1$ and B_S to establish KT melting sequence (a). String melting sequence (b) is more likely.

Figure 1 shows the string-melting possibility. The string-melting line is shown as a straight line, because Fig. 1 is only meant to be a schematic phase diagram. Actually Fig. 2 suggests a convex curve. Figure 2 also suggests that along the string-melting line, three sections can be distinguished. Close to $B=-1$ ($B=+1$), the floating phase melts into a q fluid [a $(q-1)/2$ fluid]. Close to $A=0$ it melts into an AF Potts fluid with free q-vertices but without zeros. In between it could melt directly into the Potts gas. Note however that the single-string approximation is only expected to work well close to the $B=\pm 1$ and $A=0$ axes (see Appendix). Figure 2 cannot be taken too seriously. Notice that Fig. 2 also indicates the existence of a disorder point in the AF Potts model where the Potts gas transforms into an AF Potts fluid without zeros.

To summarize, melting starts as a string-melting line at $B=\pm 1$. It is likely that the transition remains type (b) until $A=0$. The nature of the string melting may change however along the line, because the fluid changes its character (three different ones; see Fig. 2). It remains possible that string melting is replaced beyond a multicritical point close to $A=0$ by KT melting (plus a disorder line).

III. GENERALIZATION TO ODD VALUES OF $q>5$

Generalization of the $q=5$ results to $q=7,9,11,13,\ldots$ is straightforward, but increasingly obscured by the complexity of the impurities and vortices. Figure 4 shows the phase diagram for $q=7$. For $q>7$ the phase diagram remains similar. The major difference with respect to $q=5$ is that the F and AF floating phases become direct-

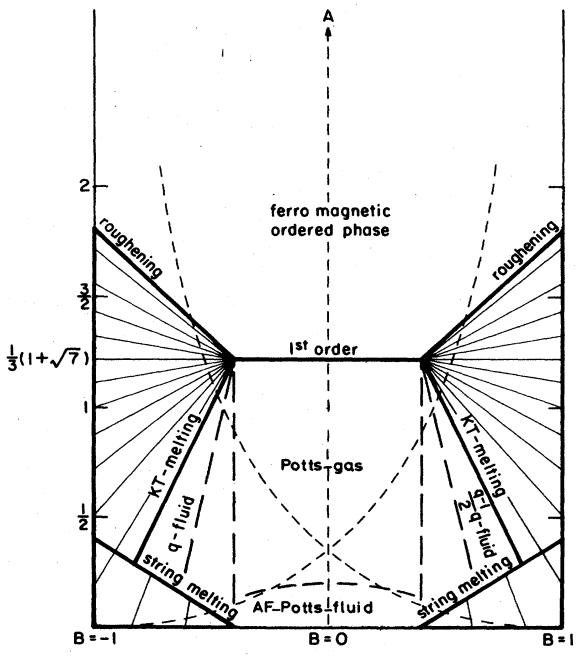

FIG. 4. Schematic phase diagram for the 7-state clock model. See caption of Fig. 1.

ly connected, possible sequence (c).

Figure 4 is a 2D interaction of a $[(q-1)/2]$-dimensional phase diagram [see Eq. (1)]. Let

$$A=x(0)/[x(1)+x(2)+\cdots+x[((q-1)/2)]\ .$$

Choose B such that, at $B=0$, $x(1)=x(2)=\cdots=x((q-1)/2)$ (the Potts model), that at $B=-1$ only $x(0)$ and $x(1)$ are nonzero (the restricted SOS model with only steps $d_h=0,\pm1$), and that at $B=1$ only $x(0)$ and $x((q-1)/2)$ are nonzero (the restricted SOS model with steps $d_h=0,\pm(q-1)/2$. The dashed lines in Fig. 4 are representative of paths where the ratios between the coupling constants $J(n)$ are fixed [see Eq. (1)]. These paths start at infinite temperature $(A,B)=(2/(q-1),0)$, and in most cases [if all $J(n)$ are negative] the $\pm(q-1)/2$ steps become dominant at low temperatures. At zero temperature $(A,B)=(0,1)$ the model reduces to the 6-vertex model.

The number of string types increases to $(q-1)/2$. The analog of Fig. 2 becomes quite complex, and varies with the actual two-dimensional intersection of the phase diagram. The vortices and impurities in different regions of the phase diagram are again composite objects of q-vertices and strings. The cores contain larger groups of linear bound q-vertices. The analog of Fig. 3 contains more complex structures. Apart from this complication the discussion of the preceding section carries over.

The ferromagnetic side of the phase diagram is similar to $q=5$. At the roughening transition the string tension of the least expensive string type vanishes: The single-arrow string tension close to $B=-1$, and the $[(q-1)/2]$-arrow string tension close to $B=1$. Depending on the actual 2D intersection of the phase diagram, a cascade of (overlapping) disorder lines could appear after the KT melting line. At each disorder line one of the remaining string tensions vanishes, and the free impurities and free vortices dissociate stepwise in a specific order. Around the points where the two critical fans close, the structure of the phase diagram may well be more complicated than shown in Fig. 4. At the first-order transition around $B=0$ all string tensions vanish simultaneously.

The important new aspect of the phase diagram is the direct connection between the ferromagnetic floating phase and the AF floating phase, i.e., the appearance of sequence (c) (see the Introduction). Recall that the ferromagnetic floating phase around $B=1$ contains logarithmically bound $q(q-1)/2$ vortices. The AF floating phase contains logarithmically bound $2q(q-1)/2$ vortices. The latter are pairs of $q(q-1)/2$ vortices, bound linearly by strings of zeros. Due to meander entropy, the string tension of the zeros vanishes again at $A_S\simeq\sqrt{2}-1$, but in contrast to $q=5$, the $q(q-1)/2$ vortices remain bound logarithmically at $A>A_S$. Recall that K increases monotonically with A (the introduction of zeros reduces the roughness) from

$$K(0,1)=[2/(q-1)]^2\pi/6$$

(the 6-vertex model) to

$$K(1,1)=[2/(q-1)]^2 0.86$$

(Luck's finite-size scaling result[10] for the restricted SOS model). Logarithmically bound $q(q-1)/2$ vortices unbind when the effective Gaussian coupling constant is larger than the universal value $K_{\rm KT}=8\pi[q(q-1)/2]^2$. At $q=7$ the relevant values of K are $K_{\rm KT}=0.057$, $K(0,1)=0.058$, and $K(1,1)=0.096$. In the absence of the strings of zeros the KT melting line would extend into the antiferromagnetic side all the way to zero temperature $(A,B)=(0,1)$. Therefore string melting sequence (b) is replaced by sequence (c). For $q>5$ close to $B=-1$ the F and AF floating solid phases are directly connected. At A_R the floating phase changes its character and has an Ising singularity in its effective Gaussian coupling constant K.

The behavior along paths where the ratios between the $J(n)$ are fixed (the dashed lines in Fig. 4), remains more speculative. As at $q=5$, K decreases with temperature, and all possible sequences (a)—(d) compete. The relevant string tensions depend strongly on the ratios of the Boltzmann weights along the actual path. The structure of the strings inside the impurities and the $2q(q-1)/2$ vortex cores is determined by these ratios. The lowest string tension determines the core size (in most cases the $d_h=\pm[(q-1)/2-1]$ strings).

Generically, the type-(c) line in the $B=1$ region first changes into a string melting line, and closer to $A=0$ (perhaps) into a KT melting line. Depending on the actual path (draw the analog of Fig. 2) several sections along the string melting line, separated by the end points of the disorder lines, might be distinguishable. At each segment another specific string tension causes the initial breakup of the vortex and impurity cores.

IV. CONCLUSIONS

The purpose of this paper is to point out the possibility of string melting of a two-dimensional floating solid phase, the divergence of the core size of impurities and vortices, and to show that this takes place in AF q-state clock models with odd values of q. A more detailed study of the singularities at string-melting transitions is in progress. The single-string approximation (see Appendix) is not sufficient since it ignores screening between strings.

The discussion of the two previous sections shows that the description of the AF q-state clock model by means of strings and vortices makes it possible to understand and/or predict the properties of the phase diagram with a minimum of exact, numerical, and analytical information. In particular it is shown that the antiferromagnetic low-temperature phase is a floating solid with composite impurities and vortices. Still both types of melting sequences (a) and (b) (see Introduction) might be realized for suitable values of the interactions. However, string melting seems more likely. Moreover, the floating solid in the AF five-state clock model certainly melts by the string-melting mechanism (b) in the SOS model regions $B=\pm1$. The new aspect in the phase diagram for $q=7,9,11,\ldots$ is that the F and AF floating phases are directly connected [sequence (c); see Introduction and Fig. 4].

Here I present two final remarks. It has been argued[12] that AF q-state clock models with odd values of q belong to the same universality class as ferromagnetic $2q$-state clock models. This is reflected by the type-(a) melting and the possibility of a low-temperature ordered phase (driven by the $\cos[4\pi h/(q-1)]$ operator) with (checkerboardlike) sublattice magnetization $\langle\theta\rangle_A=\langle\theta\rangle_B+\pi(q-1)/q$. The universality argument ignores variations in the core size and limitations to the range of the Gaussian coupling constant K in the actual model. At zero temperature (the 6-vertex model) the effective Gaussian coupling constant K takes the value $K(0,1)=[2/(q-1)]^2\pi/6$. If string melting could be ignored, then the phase diagram would be the same as for the $2q$-state clock model, but zero temperature would be located inside the intermediate floating phase of the $2q$-state clock model. This is because $K(0,1)$ is smaller than the universal value $K_R=[2/(q-1)]^2\pi/2$, where the roughening transition takes place.

The phase diagram of the AF 3-state clock model has already been discussed elsewhere.[13] The model is disordered at all $T>0$. The positional entropy is already larger than at the KT melting transition ($K(0)=[2/(q-1)]^2\pi/6$ is smaller than $K_{\rm KT}=8\pi/[(q-1)q]^2$). K increases if ferromagnetic next-nearest-neighbor interactions are introduced. Indeed we found a so-called critical fan and type-(a) melting. The string melting possibility only plays a role for values of the fugacity around a critical value where we found that the critical fan might close.

Monte Carlo renormalization results for the AF 5-state clock model[14] seem to be in agreement with Fig. 1, but additional numerical evidence for the proposed phase diagrams is needed. It must be realized however that for increasing q the impurities and vortices become increasingly more complex and larger. Only at length scales larger than the core size is the floating phase a meaningful concept. Finite-size effects become increasingly important.

ACKNOWLEDGMENT

It is a pleasure to thank Eberhard Riedel, and Gilson Carneiro, during his stay at the University of Washington, for many helpful discussions. Monte Carlo results for the 5-state clock model (Baltar, Pol, Zagury, and Carneiro[14]) started this study. This research is supported by the National Science Foundation under Grant No. DMR 83-19301.

APPENDIX

The purpose of this appendix is to obtain an estimate for the temperature dependence of the string tension. The free energy of one isolated string can be calculated via the transfer-matrix method. Assume that the string follows the bonds of a square lattice, and let z be the fugacity of the string per unit length with respect to the free energy of the surrounding phase. The partition function $Z(n,t)$ of a string which runs between site (n_0,t_0) and $(n+n_0,t+t_0)$ satisfies the recursion relation

$$Z(n,t)=z\left[Z(n,t)+\sum_{m=-\infty}^{\infty} z^{|m|}Z(n+m,t-1)\right]. \quad \text{(A1)}$$

In this approximation the string is not allowed to bend backwards in "time" t. The transfer matrix is equivalent to the time evolution of a single fermion in the one-dimensional tight-binding model. Villain[15] used the same approximation in the context of commensurate-incommensurate transitions, to model meander fluctuations in a honeycomb network of domain walls. The Fourier transform

$$Z(n,t)=\frac{1}{2\pi}\int_{-\pi}^{\pi} Z(k,t)\exp(ikn)dk \quad \text{(A2)}$$

gives the eigenmodes

$$Z(k,t+t_0)=\exp[-f_S(k)t]Z(k,t_0)\,, \quad \text{(A3)}$$

with the decay rates

$$f_S(k)=\ln\left[Z\frac{1-z^2}{1+z^2-2z\cos(k)}\right]. \quad \text{(A4)}$$

The slowest decaying mode $k=0$ determines the string tension of the string, and its average length $l_S=1/f_S(0)$. String melting takes place when the meander entropy exceeds the energy. At the string-melting transition,

$$z_S=\sqrt{2}-1\,, \quad \text{(A5)}$$

the $k=0$ mode does not decay anymore, $f_S(0)=0$. Above the string-melting temperature the string is infinitely long. Up to $z=0.3$ the string length l_S remains less than two lattice constants. Therefore all the composite vortices and impurities in the clock model have their minimum size (with the strings as short as possible) until reduced temperatures of the order of $(z-z_S)/z_S=-0.25$.

On the one hand, the single-string approximation underestimates the meander entropy, because it neglects backbending of the string. On the other hand, it overestimates the entropy, because it neglects Pauli exclusion from other strings.

The next-best approximation, which takes both effects into account, is the Ising model. Its droplet excitations form closed loops of strings (Bloch walls). The string between two vortices is described by the Bloch wall between two dislocations in the dislocation pair correlation function (dual to the spin-spin correlation function).

The Ising model approximation does not change the results. Its critical temperature is still given by (A5), and the string tension (mass gap) vanishes linearly ($y_T=1$).

The Ising approximation still ignores the response of the sea of favorable arrow states to the presence of the strings. In the floating solid phase this response can be described by effective interactions between the strings. The leading one is a pair interaction with a R^{-4} distance behavior. This is believed to be sufficiently short range not to change the critical behavior of the Ising model (see, e.g, Pfeuty and Toulouse[16]).

Notice that the vertices inside the impurity and vortex cores already deconfine when f_S^2 becomes of the same order of magnitude as the density of impurities and vortices (screening). The details of the thermodynamic singularities at the string-melting transition itself are not described by this model. (The Ising model with finite fugacity of open strings is dual to the Ising model in a magnetic field and has no phase transition.)

[1]J. M. Kosterlitz and D. J. Thouless, J. Phys. C **6**, 1181 (1973).
[2]J. M. Kosterlitz, J. Phys. C **7**, 1046 (1974).
[3]J. Jose, L. P. Kadanoff, S. Kirkpatrick, and D. R. Nelson, Phys. Rev. B **16**, 1217 (1977).
[4]J. P. van der Eerden and H. J. F. Knops, Phys. Lett. **66A**, 334 (1978).
[5]R. J. Baxter, J. Phys. C **6**, L445 (1973).
[6]S. Elitzur, R. Pearson, and J. Shigemitsu, Phys. Rev. D **19**, 3698 (1979).
[7]V. Mizrahi and E. Domany, Phys. Rev. B **24**, 4008 (1981).
[8]J. M. Luck, J. Phys. (Paris) Lett. **42**, L275 (1981).
[9]H. J. F. Knops, Phys. Rev. Lett. **39**, 766 (1977).
[10]Value quoted in J. M. Luck, S. Leibler, and B. Derrida, J. Phys. (Paris) **44**, 1135 (1983).
[11]See, e.g., M. P. M. den Nijs, J. Phys. A **12**, 1857 (1979), and references quoted therein.
[12]J. L. Cardy, Phys. Rev. B **24**, 5128 (1981).
[13]M. P. M. den Nijs, P. Nightingale, and M. Schick, Phys. Rev. B **26**, 2490 (1982).
[14]V. L. V. Baltar, M. E. Pol, N. Zagury, and G. Carneiro, J. Phys. A (to be published).
[15]J. Villain, Surf. Sci. **97**, 219 (1980).
[16]P. Pfeuty and G. Toulouse, *Introduction to the Renormalization Group and Critical Phenomena* (Wiley, New York, 1977).